

Evolutionary Type-2 Fuzzy Blood Gas Models for Artificially Ventilated Patients in ICU

S. H. Indera-Putera and M. Mahfouf

Department of Automatic Control and Systems Engineering, The University of Sheffield, U.K.

Keywords: Type-2 Fuzzy Modelling, Optimization, Blood Gases.

Abstract: This paper proposes a new modelling and optimization architecture for improving the prediction accuracy of arterial blood gases (ABG) in the SOPAVent model (Simulation of Patients under Artificial Ventilation). The three ABG parameters monitored by SOPAVent are the partial arterial pressure of oxygen (PaO_2), the partial arterial pressure of carbon-dioxide (PaCO_2) and the acid-base measurement (pH). SOPAVent normally produces the initial ABG predictions and also the ABG predictions after any changes in ventilator settings are made. Two of SOPAVent's sub-models, namely the relative dead-space (K_d) and the carbon-dioxide production (VCO_2) were elicited using interval type-2 fuzzy logic system. These models were then tuned using a new particle swarm optimization (nPSO) algorithm, via a single objective optimization approach. The new SOPAVent model was then validated using real patient data from the Sheffield Royal Hallamshire Hospital (UK). The performance of the new SOPAVent model was then compared with its previous version, where K_d and VCO_2 were modeled using a neural-fuzzy system (ANFIS). For the initial ABG predictions, significant improvements were observed in the mean absolute error (MAE) and correlation coefficient (R) for PaCO_2 and pH. When the ventilator settings were changed, significant improvements were observed for the prediction of pH and other improvements were also observed for the prediction of PaCO_2 .

1 INTRODUCTION

Mechanical ventilation is the main life support system in the intensive care unit (ICU). Clinicians optimize ventilator settings to ensure appropriate oxygenation of patients, and at the same time, to prevent risks of ventilator induced lung injuries. Changes in ventilator settings can affect blood gas parameters in as-early-as 30 minutes. However, arterial blood gases (ABG) sampling is only carried out every several hours. Sampling is also invasive and often cause discomfort to patients. Therefore, a non-invasive, and automatic ABG prediction tool is essential to assist clinicians with optimal ventilator management strategy.

SOPAVent (Simulation of Patients under Artificial Ventilation) (Figure1) is a mathematical model that simulates the human respiratory system under artificial ventilation. It was first developed by Goode (2001). The objective of SOPAVent is to predict ABG parameters of partial arterial pressure of oxygen (PaO_2), partial arterial pressure of carbon-dioxide (PaCO_2) and the acid-base measurement (pH). SOPAVent is also integrated with neural-fuzzy advisory models, which provide decision support for

ventilator settings as described by Kwok et al., (2004), Wang et al., (2010) and Mohamad-Samuri et al., (2011). Inputs to the SOPAVent system consists of routine ICU data as follows:

- i) Ventilator settings and ventilator monitoring: Positive-end expiratory pressure (PEEP), respiratory rate (RR), inspiratory pressure (P_{insp}), minute volume (MV), inspiratory to expiratory ratio (IE ratio), fraction of inspired oxygen (FiO_2), minute volume (MV) and tidal volume (V_t).
- ii) ABG analyses: PaO_2 , PaCO_2 , pH and oxygen saturation (SpO_2), and,
- iii) Patient's physiological information: Height, weight, blood pressure, airway pressure, body temperature and end-tidal carbon-dioxide production (EtCO_2).

To accurately represent the human respiratory system, SOPAVent also uses parameters that are not regularly measured in the ICU. These parameters are the relative dead-space (K_d), carbon-dioxide production (VCO_2), shunt, cardiac output (CO), and oxygen consumption (VO_2).

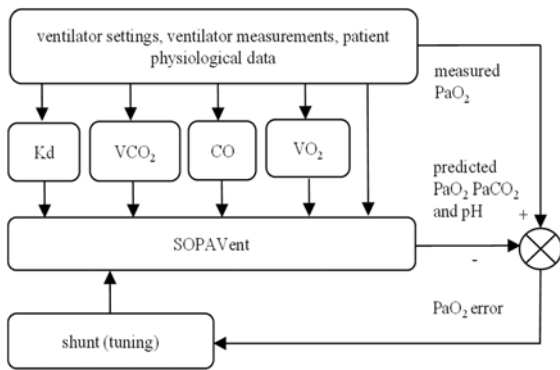


Figure 1: SOPAVent.

Several efforts have been devoted to the modelling of VCO_2 and Kd . In SOPAVent v.1, Goode (2001) tuned Kd so the predicted $PaCO_2$ matches the measured $PaCO_2$. VCO_2 was obtained using a metabolic computer. In SOPAVent v.2, Kwok et al., (2004) proposed a fuzzy model for Kd . VCO_2 was estimated using mean population. In SOPAVent v.3, Wang et al., (2010) modelled Kd and VCO_2 using artificial neural-fuzzy systems (ANFIS) and tuned the models using a hybrid Levenberg-Marquardt and back-propagation algorithm.

Indera-Putera et al., (2016) proposed a new interval type-2 fuzzy logic system (IT2 FLS) for modelling Kd and VCO_2 (Figure 2). Type-2 fuzzy logic is an approach normally used in systems with high levels of uncertainty. Type-2 membership functions which are in itself fuzzy allows for a robust and adaptable model suitable for handling complex input-output relationships (Wu, 2012). An example of an IT2 FLS fuzzy set is shown in Figure 3. Each membership function is defined by a footprint of uncertainty (FOU), which is the area between the lower membership function (LMF) and upper membership function (UMF).

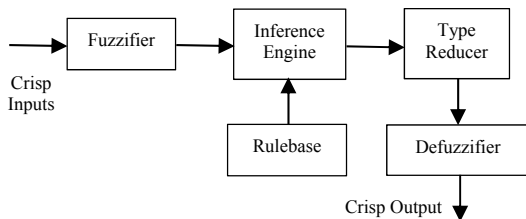


Figure 2: Type-2 Fuzzy Logic System.

The IT2 FLS in this work employs a singleton fuzzifier and a Takagi-Sugeno-Kang (TSK) consequent rule-base. The outputs were calculated using the Karnik-Mendel algorithm, as defined in Wu and Mendel (2009). The inputs used for Kd are $PaCO_2$, RR, V_t , P_{insp} and PEEP. A total of 44 fuzzy

rules were generated to map the inputs to Kd (Figures 4-5). The inputs used for VCO_2 model are V_t , MV and $EtCO_2$. A total of 27 fuzzy rules were generated to map the inputs to VCO_2 (Figures 6-7).

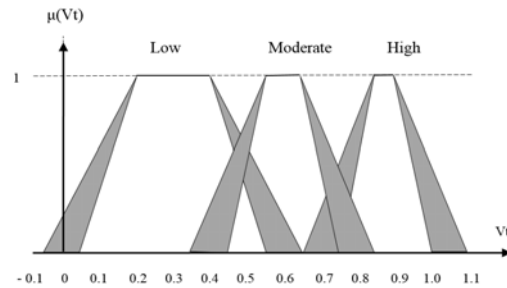


Figure 3: Membership function for an internal type-2 fuzzy logic system (Indera-Putera et al., 2016).

Inputs were selected using sensitivity analyses described by Goode (2001) and Wang et al., (2010). All membership functions (MFs) and rules were manually tuned.

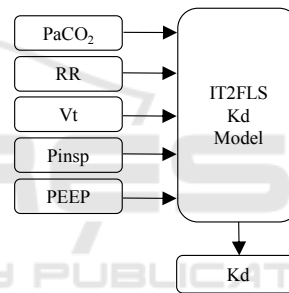


Figure 4: The IT2 FLS Kd model.

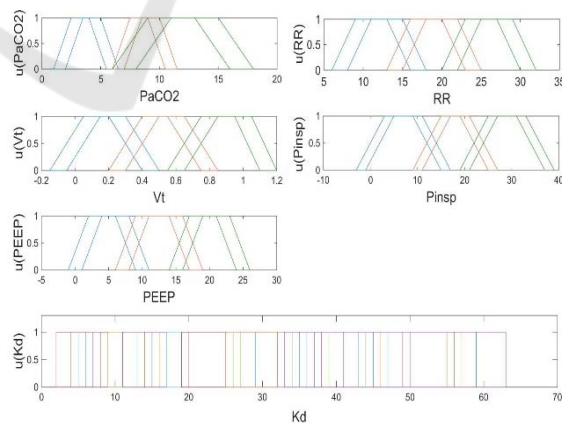


Figure 5: The IT2 FLS Kd model fuzzy set.

This paper proposes to optimize the Kd and VCO_2 models, and to validate their performances once these are integrated in the latest version of SOPAVent, SOPAVent v.4.

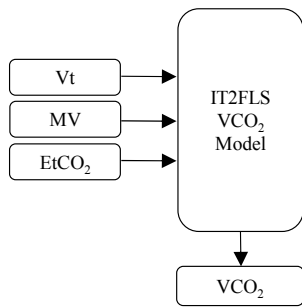


Figure 6: The IT2 FLS VCO₂ models.

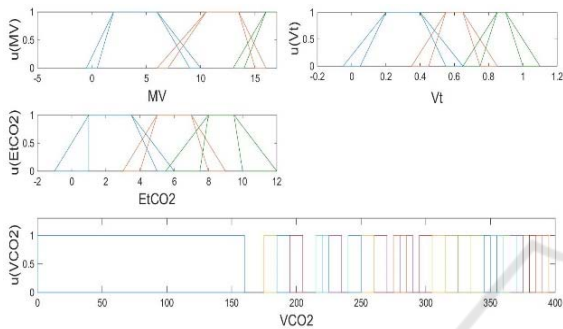


Figure 7: The IT2 FLS VCO₂ model fuzzy set.

2 OPTIMIZATION OF KD AND VCO₂ MODELS

2.1 New Particle Swarm Optimization

Particle swarm optimization (PSO) mimics the behaviour of flocking birds, also known as “particles”. Each particle has knowledge of the best location for resources through its own experience, and shares this information with other particles in the swarm. Each particle then adjusts its speed and direction in order to get to that best location. This optimal location is known as the “global best solution”.

In this work, a new PSO algorithm (nPSO) by Zhang et al., (2006) was used to further improve the prediction accuracy by optimizing the output MFs of Kd and VCO₂ models (Figure 8). The algorithm used “momentum weight” which varies depending on the particle’s current position and velocity. The maximum velocity (V_{max}) was used to contain the particle within a specified search area as follows:

$$v_{id}(t+1) = [w_{id}(t+1)*r_1*(t+1)v_{maxi}] + [c_1*r_2(t+1)*[p_{id}(t) - x_{id}(t)] + c_2*r_3(t+1)*[p_{gd}(t) - x_{id}(t)]] \quad (1)$$

$$x_{id}(t+1) = x_{id}(t) + v_{id}(t+1) \quad (2)$$

$$w_{id}(t+1) = \begin{cases} 1, & \text{if } V_i(t) \leq \mathcal{E} * V_{max} \\ & \text{and } pos_{id}(t+1) = 1; \\ w_{id}(t) * m_1, & \text{If } (\text{not } V_i(t) \leq \mathcal{E} * V_{max} \\ & \text{and } f(X_i(t) \geq f(P_i(t-1))); \\ w_{id}(t) * m_2, & \text{if } (\text{not } V_i(t) \leq \mathcal{E} * V_{max} \\ & \text{and } f(X_i(t) < f(P_i(t-1))) \end{cases} \quad (3)$$

$$m_1 < 1 \text{ and } m_2 > 1 \quad (4)$$

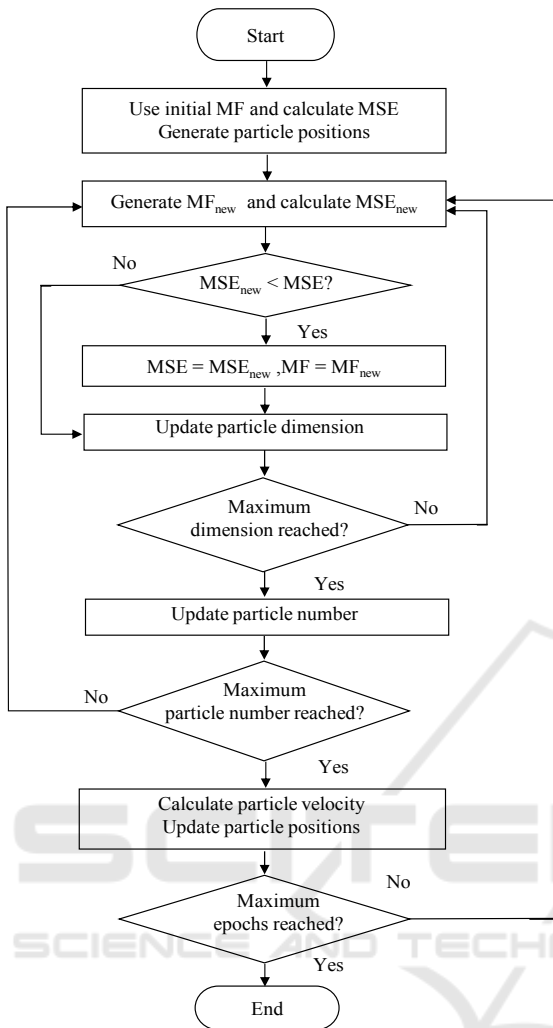
Here, i is particle number and d is the dimension, v_{id} is the velocity or change in particle position within its search area, w is the momentum weight, r_1 , r_2 and r_3 are random variables between 0 and 1, V_{max} is the maximum velocity, x_{id} is the particle position, c_1 and c_2 are acceleration constants, m_1 and m_2 are scaling parameters, \mathcal{E} is a positive coefficient and pos_{id} is a discrete variable (0 or 1).

The objective of nPSO is to return the output fuzzy set that produced the least mean squared error (MSE) as the global best solution. The nPSO dimension is determined by the number of output MFs multiplied by two; each representing the LMF and UMF of every MF in the fuzzy set.

The relative dead-space (Kd) with 44 output MFs has a particle dimension of 88. The carbon-dioxide production (VCO₂) with 27 output MFs has a particle dimension of 54. The fuzzy sets were tested on the models until the maximum epoch was reached. The nPSO algorithm then returned the fuzzy set with the least MSE. The initialising parameters for nPSO are shown in Table 1. An example of the nPSO optimization result for Kd output MF is shown in Table 2.

Table 1: nPSO Initialization.

Parameter	Value
c_1, c_2	1.8, 1.8
m_1, m_2	0.5, 2
dimensions	88, 54
V_{xar}	data range
V_{max}	$0.5V_{xar}$
epoch	30
r_1	[0, 1]
r_2	[0, 1]
r_3	[0, 1]



MF = Membership Function, MSE = mean squared error

Figure 8: nPSO flowchart for MF selection.

Table 2: Optimization Result for Kd output MF.

Output MF	Manually tuned MF		nPSO Tuned MF	
	LMF	UMF	LMF	UMF
Y1	6	36	11.95	26.76
Y2	11	41	1.94	56.03
Y3	6	36	6.30	31.59
...
...
Y42	19	49	27.92	47.64
Y43	25	55	23.86	49.23
Y44	33	63	28.57	62.57

2.2 Validation of Kd and VCO₂ Models using Real Patient Data

The data used for validation of the optimization algorithm was obtained from the Sheffield Royal Hallamshire Hospital, United Kingdom and approved

by the Research Ethics Committee (Table 3 and 4). A set of 447 data from 25 patients was available for Kd modelling and a set of 764 data from 21 patients was available for VCO₂ modelling.

A set of 230 data was randomly selected for optimization of Kd, and a set of 254 data was randomly selected for optimization of VCO₂. The optimized Kd model was validated using 68 data from 13 patients and VCO₂ model was validated using 82 data from 5 patients. Results for Kd and VCO₂ predictions were then compared with the manually tuned models.

Table 3: Kd Data Summary.

Parameter	Kd modelling data			
	mean	s.d.	min	max
PaCO ₂ (kPa)	5.72	1.10	3.82	10.1
RR (breath/min)	17.06	3.35	12	28
Vt (l)	0.52	0.12	0.29	0.88
Pinsp (cmH ₂ O)	13.98	3.68	6	30
PEEP (cmH ₂ O)	11.13	3.91	5	20
Kd	28.13	6.65	14	48
Parameter	Kd validation data			
	mean	s.d.	min	max
PaCO ₂ (kPa)	5.39	0.84	3.74	7.62
RR (breath/min)	16.21	4.19	12	28
Vt (l)	0.47	0.11	0.17	0.75
Pinsp (cmH ₂ O)	13.30	3.23	8	20
PEEP (cmH ₂ O)	9.01	2.87	5	15
Kd	29.10	7.37	14	50

Table 4: VCO₂ Data Summary.

Parameter	VCO ₂ modelling data			
	mean	s.d.	min	max
MV (l/min)	7.76	1.68	4.09	15.55
Vt (l)	0.54	0.09	0.29	0.9
EtCO ₂ (kPa)	4.80	0.97	3.18	8.51
MV (l/min)	7.76	1.68	4.09	15.55
Parameter	VCO ₂ validation data			
	mean	s.d.	min	max
MV (l/min)	8.90	1.79	5.66	15.55
Vt (l)	0.54	0.07	0.39	0.65
EtCO ₂ (kPa)	4.68	0.69	3.38	6.39
MV (l/min)	217.75	33.42	144.5	292

2.3 Kd and VCO₂ Prediction Results

The surface plots for the Kd model and Kd prediction curves are shown in Figure 9. Prediction results for Kd are shown in Tables 5-6. The optimized Kd model has reduced the number of predictions outside of the ±10% margin of error. However, some predictions were slightly higher than the actual measurements. The new model has reduced the overshooting error that exists when PaCO₂ is between 8.0kPa and 8.18kPa, and when PEEP is between 16cmH₂O and 20cmH₂O.

There still exist ‘plateaus’ in the lower regions of PaCO₂ which relates to the middle and upper regions of PEEP. This is likely due to the existing fuzzy rules which were unable to represent the entire range of inputs. A revised type-2 fuzzy model for Kd is proposed to overcome this problem.

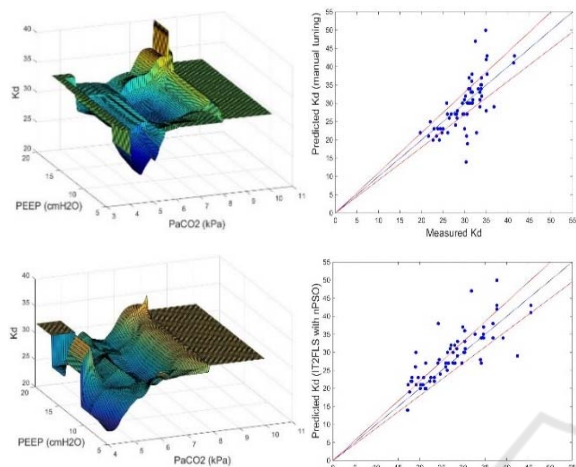


Figure 9: Surface plot and prediction curve for Kd model, (top) manually tuned model, and (bottom) nPSO tuned model.

In Kd modelling data set, the optimized model has reduced the MSE from 19.61 to 14.47 (26.21% improvement). It has also increased the correlation from 0.79 to 0.83. In Kd validation data set, the optimized model has reduced the MSE from 28.91 to 22.39 (22.55% improvement). It has also increased the correlation from 0.69 to 0.80.

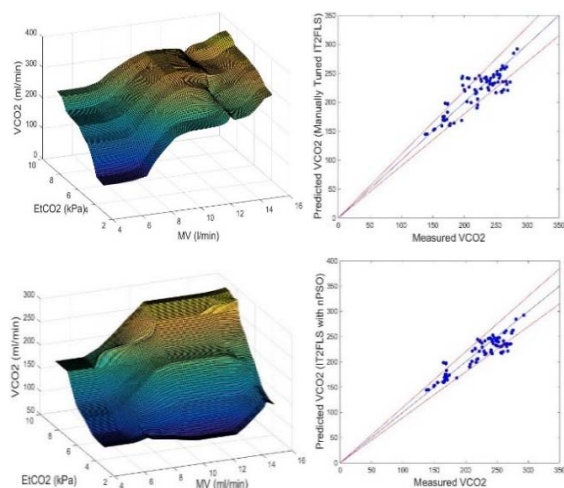


Figure 10: Surface plot and prediction curve for VCO₂ model, (top) manually tuned model, and (bottom) nPSO tuned model.

The surface plots for the VCO₂ model and VCO₂ prediction curves are shown in Figure 10. Prediction results for VCO₂ are shown in Tables 7-8. The optimized VCO₂ model has removed the majority of predictions outside of the $\pm 10\%$ margin of error. The model has smoothed the indentation observed for MV values between 12 l/min and 14 l/min. A plateauing effect can be seen on the upper region of the input, this is due to limitations of the lungs to produce carbon-dioxide (CO₂) more than its maximum capacity.

In VCO₂ modelling data set, the new VCO₂ model has reduced the MSE from 629.97 to 476.85 (24.30% improvement). It has also increased the correlation significantly from 0.79 to 0.92. In VCO₂ validation data set, the optimized model has reduced the MSE from 395.72 to 315.46 (20.28% improvement). It has also increased the correlation from 0.84 to 0.91.

Table 5: Kd Results (Modelling Data).

Tuning	MSE	MAE	s.d	R	
Manual	19.61	13.45	4.10	0.79	
nPSO cycle	1	14.47	10.92	3.81	0.83
	2	20.99	14.53	4.37	0.76
	3	15.11	11.48	3.85	0.82
	4	14.29	11.23	3.76	0.83
	5	16.71	12.17	4.05	0.80
	6	16.61	12.40	4.04	0.80

Table 6: Kd Results (Validation Data).

Tuning	MSE	MAE	s.d	R	
Manual	28.91	14.62	5.35	0.69	
nPSO cycle	1	22.39	10.98	4.53	0.80
	2	27.26	14.35	5.26	0.73
	3	23.92	13.63	4.90	0.75
	4	22.09	13.35	4.69	0.77
	5	24.64	13.68	4.98	0.74
	6	22.32	13.23	4.74	0.77

Table 7: VCO₂ Results (Modelling Data).

Tuning	MSE	MAE	s.d	R	
Manual	629.97	9.65	25.11	0.88	
nPSO cycle	1	510.03	8.13	22.62	0.91
	2	501.64	8.52	22.31	0.91
	3	463.26	8.17	21.55	0.91
	4	476.85	7.96	21.88	0.92
	5	507.83	8.49	22.50	0.91
	6	612.70	9.23	24.80	0.89

Table 8: VCO₂ Results (Validation Data).

Tuning	MSE	MAE	s.d	R	
Manual	395.72	6.98	19.86	0.84	
nPSO cycle	1	344.40	6.36	17.74	0.89
	2	384.26	6.96	18.10	0.88
	3	373.56	6.91	18.64	0.87
	4	315.46	6.33	16.60	0.91
	5	369.05	6.88	17.45	0.90
	6	311.59	6.37	16.79	0.91

2.4 Revision of the Dead-Space (Kd) Model

The type-2 fuzzy model for Kd was revised to include all possible combinations of input membership functions to form the fuzzy rules. The Kd model has five inputs and three MFs for each input. This resulted in 243 manually tuned rules for the revised fuzzy model. The revised model appears to have removed the plateauing effect and the ‘peaks’ at the higher region of the input parameters (see Figure 11).

The overall performance of the revised Kd prediction was reduced when compared to the nPSO optimized model (Table 9). This is mainly due to the fact that the fuzzy sets and rules were manually selected. The following section will discuss the revised model’s performance when integrated into SOPAVent v.4.

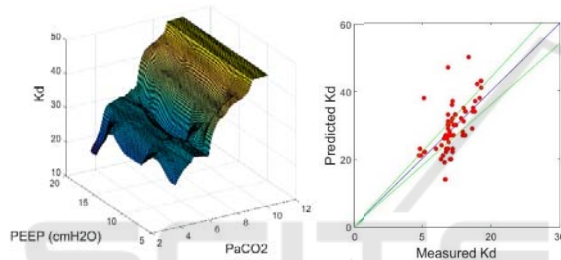


Figure 11: Surface plot for revised Kd model.

Table 9: Result for Kd Revised Model.

Data Set	MSE	MAE	s.d	R
Modelling	21.76	14.48	4.53	0.74
Validation	32.76	14.96	5.76	0.62

3 VALIDATION OF SOPAVENT BLOOD GAS PREDICTION ON REAL PATIENT DATA

The Kd and VCO₂ models were integrated into SOPAVent to create the latest version, SOPAVent v.4. In combination with the other inputs, SOPAVent v.4 will predict the ABG parameters of PaO₂, PaCO₂ and pH. The predicted ABG parameters were compared with actual ABG measurements. Two types of output were generated by SOPAVent: i) the initial ABG prediction and, ii) the ABG prediction after settings changes were applied to the ventilator. Data processing protocol, as defined in Goode (2001) and Wang et al., (2010), was also used for this research. This included the following:

- The patients were ventilated under Bi-level Positive Airway Pressure mode (BiPAP)
- The ABG samples were taken no less than 30 minutes and no longer than 60 minutes before ventilator settings were changed. ABG samples were taken at least 30 minutes but no longer than three hours after ventilator settings were changed
- The mean blood pressure variance between pre-ventilator-changes and post-ventilator-changes were within $\pm 15\%$, and
- The patient’s spontaneous breathing to total breathing ratio between pre-ventilator-changes and post-ventilator-changes were less than $\pm 15\%$

A total of 29 data sets from 21 patients were used to validate SOPAVent v.4. The patients included 14 males and 7 females with a mean weight of 70.4 ± 16 kg, a mean height of 170 ± 9.18 cm, and a mean age of 58 ± 13 years (Table 10). SOPAVent v.4 results were compared with SOPAVent v.3 by Wang *et.al* (2010). SOPAVent v.4 results are categorized across two versions of SOPAVent:

- i) SOPAVent v.4.1 with nPSO optimized Kd and nPSO optimized VCO₂
- ii) SOPAVent v.4.2 with revised Kd and nPSO optimized VCO₂

Table 10: Patient Demography.

Age	Height (cm)	Weight (kg)	Male	Female
58 \pm 13	170 \pm 9.18	70.4 \pm 16	14	7

3.1 SOPAVENT Validation Result

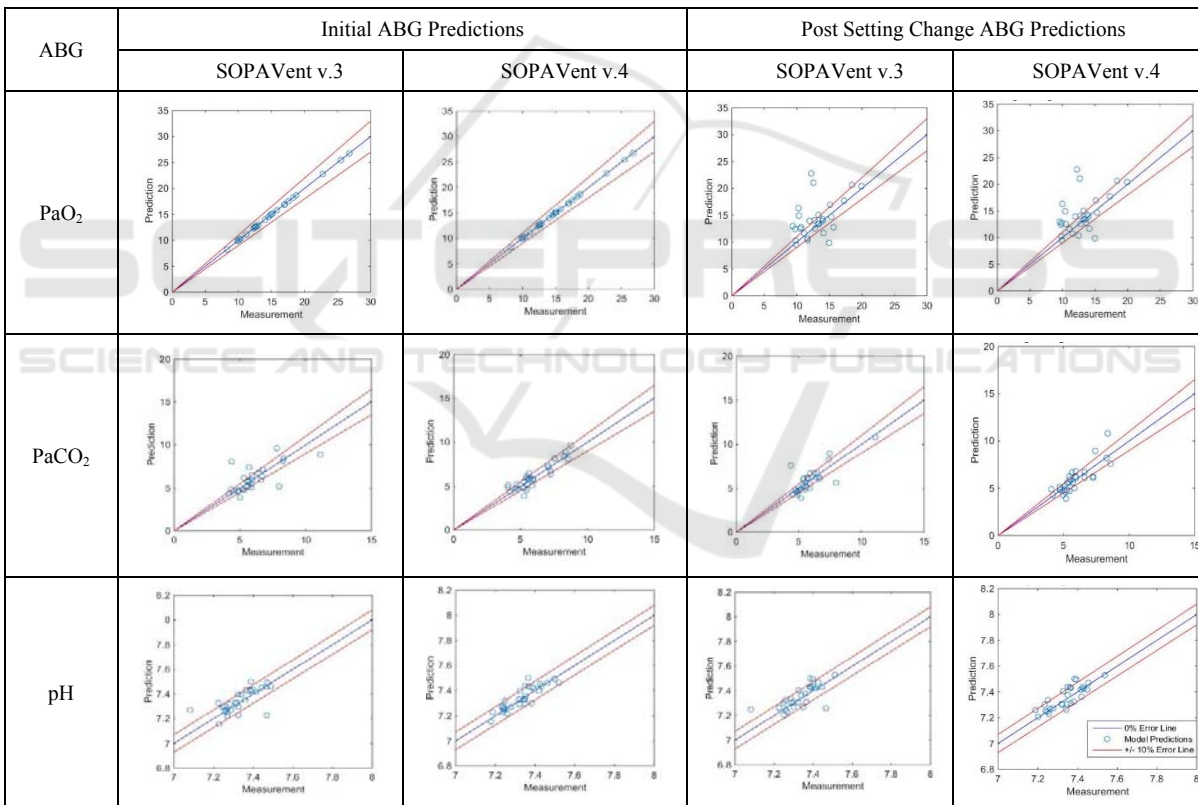
The results for SOPAVent v.4 versus SOPAVent v.3 are shown in Table 11. The comparison of performance between SOPAVent v.4 and SOPAVent v.3 is shown in Table 12.

For initial ABG prediction, both SOPAVent v.4 and SOPAVent v.3 showed identical performance for PaO₂ prediction with a correlation coefficient between modelled and measurement maintained at 1. For PaCO₂ prediction, SOPAVent v.4 has reduced the mean absolute error (MAE) from 11.60 to 9.11 (21.46% improvement) and increased the correlation significantly from 0.69 to 0.91. The majority of the predictions were within the $\pm 10\%$ margin of error. For pH prediction, the MAE was reduced from 0.71 to 0.54 (23.94% improvement) and correlation coefficient increased significantly from 0.67 to 0.88. Most predictions were within the $\pm 10\%$ margin of error.

Table 11: Initial and Post-Ventilator-Change ABG Prediction Results.

Parameter	Initial ABG Prediction				Post-Ventilator-Change ABG Prediction			
	PaO ₂				PaO ₂			
Version	MSE	MAE	s.d	R	MSE	MAE	s.d	R
v.3.0	1.14e-5	1.68e-2	3.30e-3	1.00	11.41	15.07	3.17	0.49
v.4.1	1.92e-05	2.35e-2	4.30e-3	1.00	11.44	15.18	3.14	0.50
v.4.2	1.92e-5	2.66e-2	4.20e-3	1.00	13.30	14.94	3.12	0.50
Parameter	PaCO ₂				PaCO ₂			
Version	MSE	MAE	s.d	R	MSE	MAE	s.d	R
v.3.0	1.30	11.60	1.16	0.69	0.87	10.68	0.95	0.78
v.4.1	0.64	9.85	0.76	0.86	1.09	10.11	1.03	0.74
v.4.2	0.39	9.11	0.63	0.91	0.74	10.31	0.87	0.81
Parameter	pH				pH			
Version	MSE	MAE	s.d	R	MSE	MAE	s.d	R
v.3.0	5.60e-3	0.71	7.50e-2	0.67	4.70e-3	0.69	6.80e-2	0.71
v.4.1	2.70e-3	0.57	5.28e-2	0.84	3.4e-3	0.60	5.95e-2	0.78
v.4.2	2.5e-3	0.54	4.82e-2	0.88	3.00e-3	0.59	5.15e-2	0.84

Table 12: Performance Comparison for SOPAVent v.3 and SOPAVent v.4.



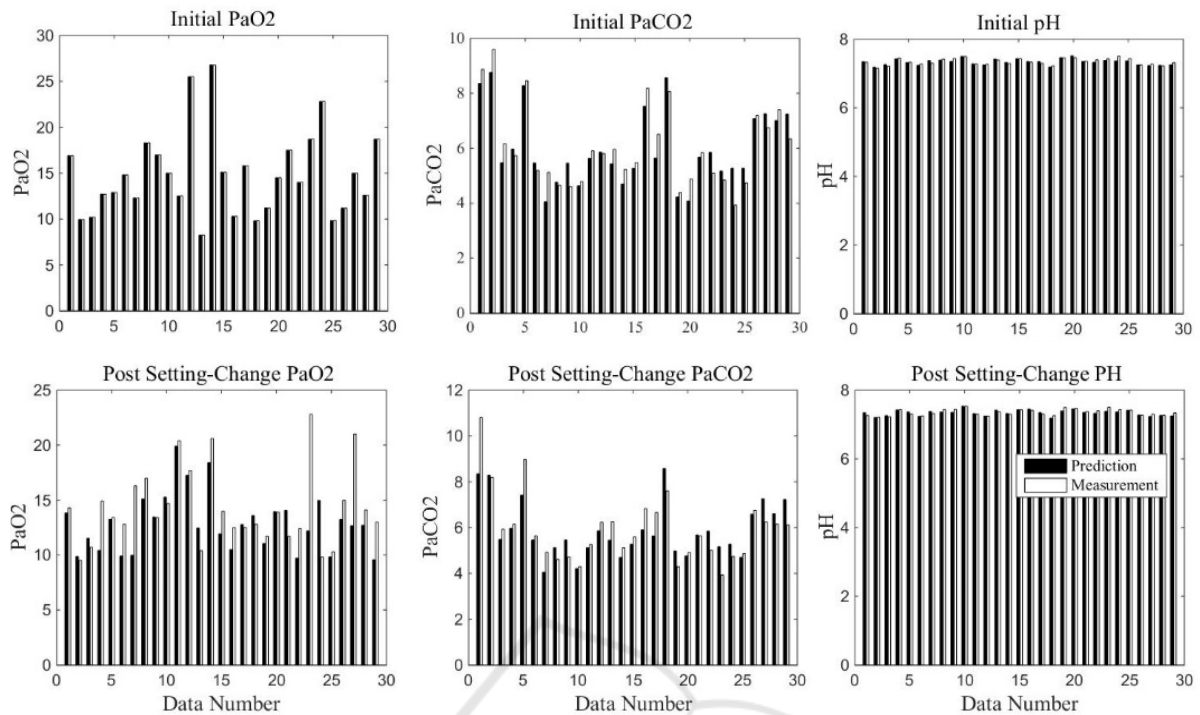


Figure 12: SOPAVent v.4 results with real ABG measurements.

When ventilator settings were changed, SOPAVent v.4 did not show any noticeable improvement in the prediction of PaO_2 . The MAE between modelled and measured maintained at 15 and the correlation coefficient stayed at 0.5. A significant amount of predictions were still outside the $\pm 10\%$ margin of error. For PaCO_2 prediction, SOPAVent v.4 has marginally reduced the MAE from 10.68 to 10.31 (3.46% improvement) and increased the correlation from 0.78 to 0.81. Most of the predictions were within the $\pm 10\%$ margin of error. For pH prediction, the MAE was reduced from 0.69 to 0.59 (14.49% improvement) and correlation was increased from 0.71 to 0.84. Most predictions are within the $\pm 10\%$ margin of error.

The results for SOPAVent v.4 against real ABG measurements are also shown in Figure 12.

4 CONCLUSIONS

A new particle swarm optimization (nPSO) algorithm was used to tune the type-2 fuzzy models of Kd and VCO_2 in SOPAVent model. The nPSO tuned models were shown to produce better prediction accuracy when compared to the manually tuned models. The new ‘momentum’ term in nPSO enables the algorithm to avoid premature convergence and creates an adap-

tive search process for the particles.

The new modelling framework has smoothed the output curve for the manually tuned VCO_2 model, and partly reduced the anomalies which relate to ‘plateaus’ and ‘peaks’ in certain input range as seen in the manually tuned Kd model. To fully mitigate this irregularity, a secondary ‘revised’ Kd model was also introduced.

On its own, the nPSO Kd model exceeded the prediction accuracy of the revised Kd model. When integrated with the nPSO tuned VCO_2 model in SOPAVent, the revised Kd model provided a slightly more stable platform. This has helped to further improve the prediction accuracy of the ABG components.

Both SOPAVent version 4.1 with the nPSO tuned Kd model and SOPAVent version 4.2 with the revised Kd model exceeded the prediction accuracy of SOPAVent version 3 in several components of the ABG. This can be seen in the ABG components of initial PaCO_2 prediction, initial pH prediction and post-ventilator-change pH prediction.

Further improvements are needed though for post-ventilator-change PaO_2 predictions and post-ventilator-change PaCO_2 predictions, as both approaches were not as effective in enhancing the prediction quality. We believe that a careful modelling of the existing cardiac output (CO) structure will help to further improve ABG prediction

accuracy for the post-ventilator-change PaO₂ and post-ventilator-change PaCO₂.

ACKNOWLEDGEMENTS

The author would like to thank Majlis Amanah Rakyat (MARA) Malaysia for funding this research.

REFERENCES

- Goode, K.M. (2001), Model based development of a fuzzy logic advisor for artificially ventilated patients, *PhD thesis*, the University of Sheffield.
- Indera-Putera, S.H, Mahfouf, M., and Mills, G.H. (2016), Blood-gas modelling for artificially ventilated patients using interval type-2 fuzzy logic system, *XIV Mediterranean Conference on Medical and Biological Engineering and Computing (MEDICON)*, Cyprus.
- Kwok, H. F., Linkens, D. A., Mahfouf, M., and Mills, G. H. (2004). SIVA: A hybrid knowledge-and-model-based advisory system for intensive care ventilators, *IEEE Transactions on Information Technology in Biomedicine* 8(2): 161-172.
- Mohammad-Samuri, S., Mahfouf, M., Denaï, M., Ross, J.J. and Mills, G.H (2011), Absolute EIT coupled to a blood gas physiological model for the assessment of lung ventilation in critical care patients, *Journal of Clinical Monitoring and Computing*, Vol. 25 (1), pp. 27-28.
- Wang, A., Mahfouf, M., Mills, G.H., Panoutsos, G., Linkens, D.A., Goode, K., Kwok H.F., and Denaï, M. (2010), Intelligent model-based advisory system for the management of ventilated intensive care patients: Hybrid blood gas patient model, *Computer Methods and Program in Engineering*, Vol. 99 Issue 2, pp. 195-207.
- Wu, D. and Mendel, J.M. (2009), Enhanced Karnik-Mendel algorithms, *IEEE Transaction on Fuzzy Systems*, vol. 17, no.4, pp. 923-934.
- Wu, D., (2012), On the Fundamental Differences between Interval Type-2 and type-1 Fuzzy Logic Controllers, *IEEE Transaction on Fuzzy Systems*, vol. 20, no.5, pp. 832-848.
- Zhang, Q. and Mahfouf, M. (2006), A new structure for particle swarm optimization (nPSO) applicable to single objective and multi-objective problems, *3rd International IEEE Conference Intelligent Systems*, London, United Kingdom.

APPENDIX A

(a) O₂ transport equations in SOPAVent:

$$\frac{dCaO_2}{dt}V_a = \dot{Q}_t[XC_vCO_2 + (1-X)C_pO_2 - CaO_2] \quad A.1$$

$$\frac{dCtO_2}{dt}V_t = \dot{Q}_t[CaO_2 - CtO_2] - \dot{V}_{O_2} \quad A.2$$

$$\frac{dCvO_2}{dt}V_v = \dot{Q}_t[CtO_2 - CvO_2] \quad A.3$$

$$\frac{dCpO_2}{dt}V_p = \dot{Q}_t(1-X)[CvO_2 - CpO_2 + O_2Diff] \quad A.4$$

$$\frac{dCAO_2}{dt}V_A = RR(V_T - V_D) \left(FiO_2 - \frac{CAO_2}{1000} \right) - \dot{Q}_t(1-X)O_2Diff \quad A.5$$

$$O_2Diff = B_{O_2} \left[P_{mean} \left(\frac{CAO_2}{1000} \right) - P_pO_2 \right] \quad A.6$$

$$P_pO_2 = f_{inv}(CpO_2) \quad A.7$$

Where x is A (alveolar), a (arterial), t (tissue), v (venous) and p (pulmonary)

V _x	Volume. (l)
Q̇ _t	Cardiac output (l/min)
X	Fraction of blood shunted passed the lungs
Ṁ _{O₂}	O ₂ consumption (ml/min)
V _D	Alveolar dead-space volume (ml)
V _T	Ventilator tidal volume (ml)
RR	Respiratory rate (breath/min)
CaO ₂	Alveolar O ₂ content (ml/l)
CxO ₂	O ₂ concentration (ml/l).
B _{O₂}	O ₂ diffusion constant (ml/kPa/l)
P _{mean}	Mean airway pressure (kPa)
FiO ₂	Inspired fraction of O ₂
PpO ₂	Pulmonary partial pressure of O ₂ (kPa)
f _{inv}	Inverse of the O ₂ dissociation function

(b) CO₂ transport equations in SOPAVent:

$$\frac{dCaCO_2}{dt}V_a = \dot{Q}_t[XC_vCO_2 + (1-X)C_pCO_2 - CaCO_2] \quad A.8$$

$$\frac{dCtCO_2}{dt}V_t = \dot{Q}_t[CaCO_2 - CtCO_2] - \dot{V}_{CO_2} \quad A.9$$

$$\frac{dCvCO_2}{dt}V_v = \dot{Q}_t[CtCO_2 - CvCO_2] \quad A.10$$

$$\frac{dCpCO_2}{dt}V_p = \dot{Q}_t(1-X)[CvCO_2 - CpCO_2 + CO_2Diff] \quad A.11$$

$$\frac{dCACO_2}{dt}V_A = RR(V_T - V_D) \left(FiCO_2 - \frac{CACO_2}{1000} \right) - \dot{Q}_t(1-X)CO_2Diff \quad A.12$$

$$CO_2Diff = B_{CO_2} \left[P_{mean} \left(\frac{CaCO_2}{1000} \right) - P_pCO_2 \right] \quad A.13$$

$$P_pCO_2 = f_{inv}(CpCO_2) \quad A.14$$

- V_{CO_2} Carbon dioxide production (ml/min)
- $CaCO_2$ Alveolar CO₂ content (ml/l)
- $CxCO_2$ CO₂ concentration (ml/l).
- B_{CO_2} CO₂ diffusion constant (ml/kPa/l)
- $FiCO_2$ Inspired fraction of CO₂
- $PpCO_2$ Pulmonary partial pressure of CO₂ (kPa)
- f_{inv} Inverse of the CO₂ dissociation function

(c) O₂ dissociation function

$$C(O_2) = \beta_h \cdot Hb \cdot SO_2 + \alpha_b \cdot PO_2 \quad A.15$$

Where,

- Hb Haemoglobin concentration
- SO_2 O₂ saturation
- β_h Haemoglobin O₂ combining capacity
- α_b O₂ plasma carrying capacity

(d) CO₂ dissociation function

$$[CO_2]_{Blood} = 22.2 [CO_2]_{plasma} \{d \cdot pcv + (1 - pcv)\} \quad A.16$$

Where,

- pcv Packed cell volume (haematocrit)